Electron-spin resonance of stable radicals in Langmuir-Blodgett films of a merocyanine dye: Study of hyperfine coupling using a ^{15}N-enriched dye

Shin-ichi Kuroda, Keiichi Ikegami, Yuka Tabe, Kazuhiro Saito, Mitsuyoshi Saito, and Michio Sugi
Electrotechnical Laboratory, Tsukuba, Ibaraki 305, Japan
(Received 7 May 1990; revised manuscript received 12 September 1990)

Two kinds of stable radical species exist in mixed Langmuir-Blodgett (LB) films of a merocyanine dye and arachidic acid. One of the species exhibits clear nitrogen hyperfine structure in ESR spectra, which was previously confirmed by measurements at *X* and *Q* bands. Use of the ^{15}N-enriched dye derivative clearly identified the hyperfine coupling to arise from the nitrogen nucleus in benzothiazole, which belongs to the chromophore of the dye molecule; N—C=C—C=C—C=O. ESR spectra measured at both *X* and *K* bands in unsubstituted and ^{15}N-substituted systems permits the detailed analysis of in-plane molecular orientation using the spectrum-simulation method incorporating three-dimensional freedom of orientation. The analysis of the dependence of the spectra on the substrate position yields the local orientation of the radical molecules, which shows a higher degree of orientation toward the edge of the substrate. This behavior coincides with that of the majority of molecules forming *J* aggregates, obtained from optical analysis, and is well described by a recent theory of the flow orientation of molecular domains caused during the dipping process of LB films. This coincidence between the orientation of the radicals and *J* aggregates provides new evidence that stable radicals are generated in the *J* aggregate. The mechanism of radical generation is discussed in view of our previously proposed model of an intermolecular charge transfer in *J* aggregates.

I. INTRODUCTION

The existence of stable radical species has been demonstrated in the mixed Langmuir-Blodgett (LB) films of a merocyanine dye and arachidic acid.[1–5] The chemical structure of the dye is shown in Fig. 1 as DS and it has benzothiazole as a donor nucleus. These LB films exhibit a *J* band in the optical-absorption spectra in the as-grown state.[6] The relevence of the existence of these stable radicals to the nature of the *J* band[7] is of interest.

As reported previously,[2–5] ESP spectra of these LB films exhibit a clear anisotropy both for the in-plane and out-of-plane orientations of the film, as shown by solid curves in Fig. 2. The spectra actually contain signals from two radical species of different spin-lattice relaxation times. The saturation behavior of the ESR signal as well as the electron nuclear double resonance (ENDOR)–induced ESR spectra separated the overlapped spectra and revealed that one of the species (hereafter called species *A*) is responsible for the resolved structure of the in-plane spectra. The second radical species (hereafter called species *B*) exhibits nearly structureless broad line shapes compared with species *A*. Further, considering the preferential orientation of molecules expected from the in-plane optical dichroism,[8] the triplet structure of the higher-field side of the in-plane spectra centered at $g=2.002$ was predicted to be a nitrogen hyperfine structure of a π electron from its anisotropic behavior[2] and it was later confirmed to be the case by the

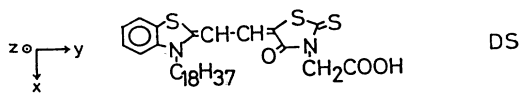

FIG. 1. Chemical structure of a surface-active merocyanine. The definition of molecular coordinate is also shown.

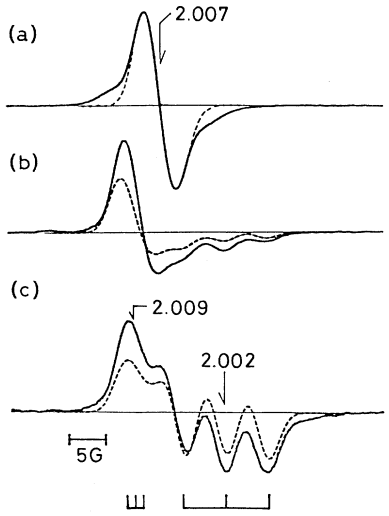

FIG. 2. Orientation dependence of the first-derivative ESR spectra of a 1000-layered DS film, prepared by manual dipping, at room temperature (solid line). The external field is normal to the film plane in (a) whereas it lies in the film plane and makes an angle of 0° and 90° with the dipping direction of the substrate for (b) and (c), respectively. The numbers show the *g* values of the fields as indicated. Dashed line shows the calculated spectra for radical species *A*. Resonance fields corresponding to the principal components of the *g* and the hyperfine tensors are shown by stick lines at the bottom of the figure.

comparison of the spectra at the X and Q bands.[3,4] At the same time, the lower-field peak at $g=2.009$ was confirmed to be associated with the g value of another principal axis (long axis) of the molecule.

Based on this fact, the ESR spectra of species A were analyzed by computer simulation to give a detailed in-plane orientation distribution function of the paramagnetic molecules in LB films: in the first step, the in-plane spectra were analyzed by considering two-dimensional freedom of orientation.[3,4] Later, we reported an improved method by incorporating three-dimensional freedom of orientation.[5] The method will be summarized later in this paper. The calculated spectra are shown by dotted curves in Fig. 2. These results reveal a characteristic orientation of the radical molecules as shown in FIg. 3. The $p\pi$ orbital of the molecule makes an average angle of $\phi_0 \approx 60°$ with the dipping direction of the substrate.[3-5] The observed orientation is consistent with the structure of the J aggregate of dye molecules, derived from optical analysis[7,9] if we assume that the radicals originate from the molecules forming J aggregates whose long axes are aligned along the dipping direction due to a flow orientation.[3-5]

Stimulated by these results, the study of flow orientation started by employing the variation of dipping speed of LB films in a wide dynamic range. A recent theoretical analysis of the flow orientation of molecular domains caused during the monolayer transfer process has successfully explained the observed flow orientation effect, which was studied through the in-plane optical dichroism of the J band.[10,11] An important theoretical prediction is that the degree of molecular orientation is dependent on the dipping velocity v_d, the width of substrate a, and the position in the substrate, due to the variation of flow forces. Recent studies of the local variation of the ESR spectra, depending on the position of the substrate of the specimens prepared with different values of v_d and a, have successfully confirmed the expected positional dependence,[12,13] which supports our proposal that the radical molecules are associated with J aggregates.

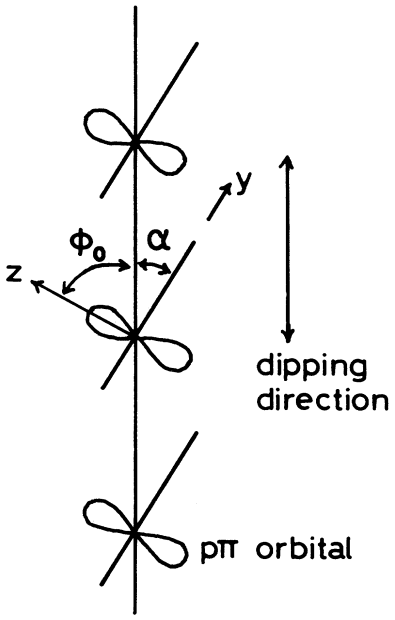

FIG. 3. Orientation of stable radical species A in the film plane. ϕ_0 denotes the angle between the $p\pi$ orbital axis (z axis in Fig. 1) and the dipping direction of the substrate. The long axis of the dye chromophore (y axis) is expressed by a thick line.

In this context, the detection of the nitrogen hyperfine structure for the spectra of species A confirms that the radical species A are associated with the π system of the dye molecule. As seen from Fig. 1, there are two nitrogen atoms in the molecule. Recently we have shown, using a ^{15}N-substituted dye derivative, that the observed nitrogen site is the one in benzothiazole (left-hand side of the molecule).[12] This nitrogen belongs to the chromophore part of the molecule, responsible for the optical properties of the system.

The hyperfine structure due to this isotope, at the same time, provides a new probe in the analysis of the ESR line shape. Here we report the confirmation of the hyperfine structure due to ^{14}N and ^{15}N in unsubstituted and substituted films, respectively, by measuring the spectra at two microwave frequencies, X and K bands. The local orientation of the radical species A is discussed from the observed spectra in ^{15}N-substituted samples to examine the detailed correlation between the orientations of radicals and those of the majority of molecules obtained by optical analysis. We also discuss our previously proposed model of intermolecular charge transfer for the mechanism of radical generation from the spectra at X and K bands.

II. EXPERIMENTAL

As for ^{15}N-substituted dye derivative, the enrichment of ^{15}N nitrogen in benzothiazole was determined by NMR to be 99.7%. Samples were prepared by the standard vertical dipping method, as described previously.[1,10,11] The substrates were sheets of polyethylene terephthalate of 0.1 mm thick.[1] For the measurement of the dependence of the spectra on the position of the substrate, the samples were cut into pieces with a width of 2 mm, to give the variation along the direction perpendicular to the dipping direction.

ESR spectra were recorded at the X band by a Varian E4 spectrometer and at the K band by a conventional homodyne spectrometer.

III. ESR SPECTRUM SIMULATION METHOD TO ANALYZE THE THREE DIMENSIONAL ORIENTATION OF RADICAL MOLECULES

The ESR spectrum simulation method has been employed for the analysis of molecular orientation in LB films.[14-16] We summarize here the simulation method incorporating the three-dimensional freedom of molecular orientation by using Eulerian angles.[5]

The ESR spectrum of a π electron radical, interacting with a nuclear spin, is well described by the following spin Hamiltonian:[17]

$$\mathcal{H}=\mu_B \mathbf{S}\cdot\overleftrightarrow{\mathbf{g}}\cdot\mathbf{H}+\mathbf{S}\cdot\overleftrightarrow{\mathbf{A}}\cdot\mathbf{I}\ . \tag{1}$$

The first term is the electronic Zeeman energy and the second term is the hyperfine coupling with a nucleus, ^{14}N or ^{15}N nucleus in the present case. **S**, **I**, and **H** denote the electron spin, nuclear spin, and the external magnetic field, respectively. $\overleftrightarrow{\mathbf{g}}$ and $\overleftrightarrow{\mathbf{A}}$ represent the **g** tensor and the hyperfine tensor, respectively.

In Fig. 1 the definition of the coordinate axes in the molecule is also shown, where we take the z axis as parallel to the $p\pi$ orbital axis. The x and y axes are taken parallel to the hydrophobic chain bonded to a nitrogen atom and the long axis of the chromophore, respectively. In this coordinate system, having $p\pi$ orbital axis as the z axis, g the hyperfine tensors become diagonal for the π electron radicals.

Figure 4 shows the Eulerian angles (θ,ϕ,ψ), in the usual notation, to define the molecular orientation. X, Y, and Z represent the coordinates fixed to the substrate, where the X axis and the Z axis are parallel to the dipping direction and the plane normal, respectively. x, y, and z are the coordinates fixed to the molecule defined in Fig. 1. θ and ϕ define the orientation of the z axis (the $p\pi$ orbital axis) for the out-of-plane and the in-plane orientations of the substrate. Rough estimation of the orientation of the z axis is readily possible from the anisotropic behavior of the triplet splitting in the spectra of Fig. 2. The ^{14}N hyperfine splitting shows a clear triplet splitting due to nuclear spin 1 along the z axis, and a much weaker splitting along the direction perpendicular to the z axis.[17] The lack of a triplet structure in the spectrum with the external field along the plane normal in Fig. 2(a) shows that the z axis is nearly confined in the film plane, that is, $\theta\approx 90°$. In this case, ψ, which shows the rotation of the y axis (the long axis of the chromophore) around the z axis, represents the out-of-plane deviation of the y axis.

The direction cosines (l_i,m_i,n_i) with $i=x$, y, or z of those molecular axes with respect to the substrate coordinate can be expressed using the Eulerian angles according to the standard procedure. When the direction cosines of the external field to the substrate are given by (L,M,N), the direction cosines (l,m,n) of the external field with respect to the molecular coordinate are expressed as

$$l=\hat{\mathbf{H}}\cdot\hat{\mathbf{x}}=Ll_x+Mm_x=Nn_x\ , \tag{2}$$

and similar expressions for m and n. Then the molecule shows the g and hyperfine coupling values given as follows:[18]

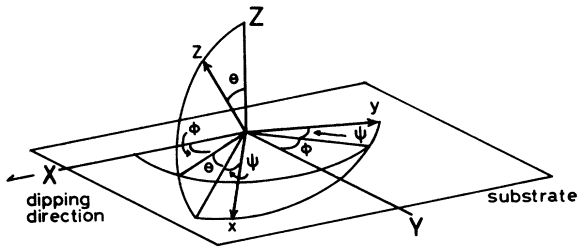

FIG. 4. Eulerian angles to define the molecular orientation in the substrate. The X, Y, and Z axes are the coordinates fixed to the substrate, where the X and Z axes are parallel to the dipping direction and the plane normal, respectively. The x, y, and z axes show the coordinate fixed to the molecule, as defined in Fig. 1.

$$g^2(\theta,\phi,\psi)=g_x^2l^2+g_y^2m^2+g_z^2n^2, \tag{3}$$

$$A^2(\theta,\phi,\psi)=A_x^2l^2+A_y^2m^2+A_z^2n^2\ . \tag{4}$$

Here g_i and A_i with $i=x,y,z$ show the principal tensor components. The resonance field for the molecule pointing (θ,ϕ,ψ) direction is given as

$$H_{\rm res}(\theta,\phi,\psi,m_I)=[h\nu-m_I A(\theta,\phi,\psi)]/g(\theta,\phi,\psi)\mu_B\ . \tag{5}$$

Here $h\nu$ shows the energy of the microwave photon. m_I is the magnetic quantum number of the nuclear spin. The magnitudes of the hyperfine couplings of ^{14}N $(I=1)$ and ^{15}N $(I=\frac{1}{2})$ nuclei are related to each other through the difference of their gyromagnetic ratios[19] as

$$A_i(^{15}N)/A_i(^{14}N)=\gamma(^{15}N)/\gamma(^{14}N)=1.403, \quad i=x,y,z\ . \tag{6}$$

Therefore, the triplet structure due to ^{14}N in Fig. 2 should be replaced by a doublet structure with the splitting 40% larger than that of the triplet upon substitution of ^{15}N.

The ESR spectrum $I(H)$ for the given orientation of the external magnetic field is obtained by summing the contributions from all orientations of molecules considering the orientation distribution as

$$I(H)=\sum_{m_I}\int_0^{\pi}\int_0^{\pi}\int_0^{\pi}F[H-H_{\rm res}(\theta,\phi,\psi,m_I)]P(\theta,\phi,\psi)\sin\theta\,d\theta\,d\phi\,d\psi\ . \tag{7}$$

Here the function F is the line-shape function, which is assumed to be Gaussian with isotropic linewidth, for simplicity. The function P is the distribution function for the molecular orientation. In our previous papers,[3,4] we have shown that the z and y axes are nearly confined in the plane $\theta\approx 90°$, $\psi\approx 0°$. Considering this point we assume that the function P can be decoupled into the product of the distribution functions of each angle, the functional form previously adopted being retained. The in-plane distribution function for ϕ, for example, becomes

$$P(\phi)\propto\exp[-\sin^2(\phi\pm\phi_0)/2\sin^2\delta]\ . \tag{8}$$

Here $\pm\phi_0$ shows the most probable orientation. δ shows the width of distribution. In the case of $P(\phi)$, the physical basis has been given by the flow orientation theory as

the Boltzmann function,[10,11] to be discussed later.

Employing the above procedure, the spectra of unsubstituted film shown in Fig. 2 could be analyzed. For g and the hyperfine tensor components, the following values were deduced from the observed g values and hyperfine splittings: $g_x=2.0068$, $g_y=2.0093$, $g_z=2.0023$, and $A_z=5.5$ G. $A_x=A_y=1.1$ G and the peak-to-peak width[20] of 3.1 G of the Gaussian function in Eq. (8) was estimated from the width of the spectrum along the plane normal in Fig. 2(a) and the widths of structures of the in-plane spectra in Figs. 2(b) and 2(c). Using those values, good agreement between the calculated spectra of species A, shown by broken lines in Fig. 2, and the observed spectra was obtained for the distribution functions of the form in Eq. (8) with the parameter values as listed below. The difference between the observed and calculated curves is due to the overlapping signal from the second radical species (species B) as mentioned above.

The in-plane distribution function parameters are $\phi_0=60°-65°$ with $\delta=25°-30°$, which are consistent with the previous estimates considering the two-dimensional degree of freedom of orientation. The average in-plane orientation of the radical molecules is schematically shown in Fig. 3.

The out-of-plane distribution parameters are $\theta_0-90°\approx 7°$ with $\delta=6°-8°$ and $\psi_0\approx 5°$ with $\delta\approx 10°$. These parameters directly characterize the deviation of the $p\pi$ orbital axis (z axis) or the long axis of the chromophore (y axis) out of the plane, which leads to the slight asymmetry of the nearly Gaussian line shape observed along the plane normal in Fig. 2(a), due to the g value distribution. The higher degree of orientation along the plane normal ($\delta=6°-8°$ for θ_0), compared with the in-plane distribution, is consistent with the lamellar structure of LB films. The long axis of the molecule is nearly confined in the plane ($\psi_0\approx 5°$), which is consistent with the results of optical absorption[8] as well as the results of electroabsorption.[21]

In the next section we extend the spectrum simulation method developed in this section to the spectra of ^{15}N-substituted films as well as the spectra taken at the K band and further examine the molecular orientation in the present system

IV. EXPERIMENTAL RESULTS AND DISCUSSION

A. ESR spectra of ^{15}N-subsituted and unsubstituted DS films at X and K bands

Figure 5 shows the comparison of ESR spectra at the X band (9.27 GHz) and the K band (24.1 GHz) for an unsubstituted DS film, prepared by manual dipping, at room temperature. The direction of the external magnetic field is the same as that for Fig. 2(c) and is parallel to the film plane and perpendicular to the dipping direction. For this direction of field, the triplet hyperfine splitting of ^{14}N along the $p\pi$ orbital axis becomes most prominent. The solid curve in Fig. 5(a) shows the spectrum at the X band, while that in Fig. 5(b) shows the spectrum of the same sample at the K band. It is seen that the triplet

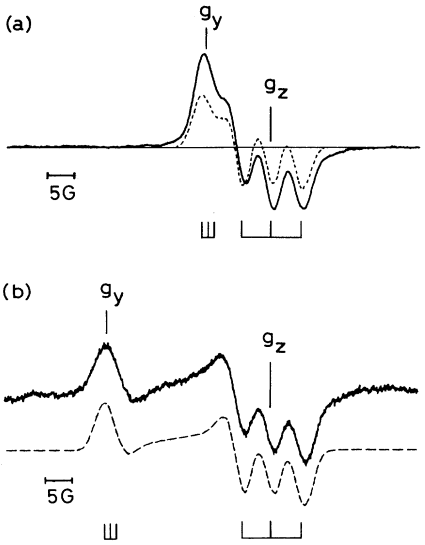

FIG. 5. Comparison of the first-derivative ESR spectra at the X band [9.27 GHz; solid curve in (a)] and the K-band [24.1 GHGz, solid curve in (b)] in a 1000-layered DS film, prepared by manual dipping. Spectra were recorded at room temperature with the microwave power 2 mW. The external field is parallel to the film plane and perpendicular to the dipping direction [the same case as Fig. 2(c)]. g_y and g_z show the g values of corresponding molecular axes. Dashed lines in (a) and (b) show the calculated spectra of species A according to the method described in Sec. III, using the common parameters of $\phi_0=60°$ and $\delta=25°$ for the in-plane distribution function of Eq. (8). Stick lines show the triplet hyperfine structure due to ^{14}N nucleus with principal g and hyperfine tensor components along the y axis (lower-field side) and the z axis (higher-field side).

hyperfine structure is retained at both frequencies, while the separation between the center of the triplet marked by g_z and the lower-field peak marked by g_y increases linearly with the microwave frequency. This is consistent with the previously reported results at the Q band, which led to our assignment of the triplet structure to the nitrogen hyperfine splitting along the z axis and the lower-field peak to the hyperfine line along the y axis of the molecule (triplet being not resolved because of the linewidth). The hyperfine structure corresponding to the principal tensor components are marked by triplet stick lines in each figure.

The dashed line in Fig. 5(a) shows the calculated curve with $\phi_0=60°$ and $\delta=25°$ with other parameters being the same as listed in the previous section. Since the spectrum at the K band is easily calculated according to the method described in Sec. III by simply changing the value of $h\nu$ in Eq. (5), the validity of the previous analysis at the X band can be crucially examined by checking whether or not the calculated spectrum of the K band, using the same values of parameters as those used in the X band simulation, reproduces the observed curve at the K band. The dashed line in Fig. 5(b) is the calculated curve. Although the spectra of species B is not yet clear

at the K band, it is seen that the observed feature of the spectra is well reproduced by the calculation, as in the case of the X band. This assures the validity of the present analysis. From these calculations, the values of $\phi_0=60°$ and $\delta=25°$ were found to be preferred to $\phi_0=65°$ and $\delta=30°$ for the data shown in Fig. 5. As to be mentioned, however, the value of ϕ_0 actually shows a certain sample dependence around $\phi_0\approx 60°$.

Figure 6 shows a similar comparison of the spectra at the X band [Fig. 6(a)] and the K band [Fig. 6(b)] in a DS film using ^{15}N-substituted dye, prepared with the conditions of $a=13$ mm and $v_d=50$ mm/min. The direction of the external magnetic field is the same as that in Fig. 5. As is clearly seen, the triplet hyperfine splitting in Fig. 5 is completely replaced by the doublet hyperfine splitting with the splitting being 40% larger than that of the triplet. This is consistent with the difference of the nuclear spin and gyromagnetic ratio of ^{14}N and ^{15}N mentioned in the previous section. Doublet stick lines show the hyperfine structure corresponding to the principal tensor components due to ^{15}N. Therefore the present results confirm that the nitrogen hyperfine coupling arises from the nitrogen nucleus in benzothiazole and hence the wave function of radical species A is directly associated with the dye chromophone which determines the electronic states of the J aggregate. This fact suggests that the generation of radical species A is intrinsically related to the nature of the J aggregate.

The dashed lines in Fig. 6 show the calculated curves at the X and K bands with $\phi_0=58.5°$ and $\delta=25°$ in this

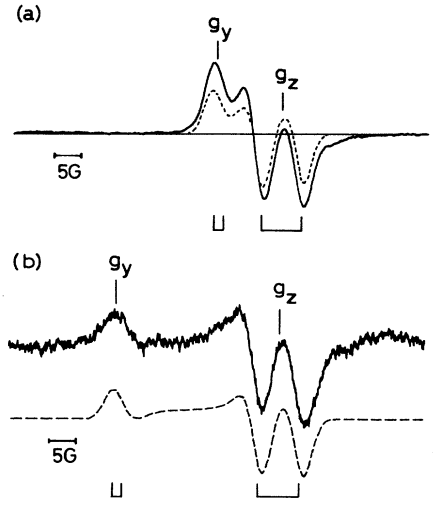

FIG. 6. Similar comparison of the first-derivative ESR spectra at the X band [solid curve in (a)] and at the K band [solid curve in (b)] as Fig. 5 in a ^{15}N-substituted DS film using dye with the nitrogen in benzothiazole (left-hand side of the molecule in Fig. 1) being 99.7% substituted by ^{15}N. The specimen is a 150-layered film prepared with the substrate width of $a=13$ mm and the dipping speed of $v_d=50$ mm/min. Calculated spectra at X and K bands use $\phi_0=58.5°$ and $\delta=25°$. Stick lines show the doublet hyperfine structure due to ^{15}N nucleus along principal axes.

case. The value of ϕ_0 is slightly smaller than that determined in Fig. 5, showing an example of the sample dependence of ϕ_0. It is also seen in this case that the same parameter values reproduce the spectra both at the X and K bands considerably well, again confirming the validity of the present analysis.

As will be discussed below in detail, the value of δ show a local variation in the substrate. On the other hand, the data shown in Figs. 5 and 6 are the spectra of the whole sample area and the values of δ cited above should be considered as effective values averaged over the whole sample area. Comparison between the observed curves and the calculated curves at the X and K bands can be similarly extended to the local spectra.

B. Locally resolved ESR spectra in ^{15}N-substituted DS films at the X band

As pointed out in Sec. I, in the case of unsubstituted DS films, the spectra showed clear dependence on the position in the substrate for the samples prepared with different values of v_d and a and the effect was quantitatively explained by the flow orientation theory.[12,13] It is therefore expected that a similar behavior can be observed in ^{15}N-substituted films.

A recently developed model of the flow orientation of monolayers during the dipping process[10,11] provides the physical basis for the distribution function in Eq. (8). In this model, the monolayer and the substrates are approximated by a two-dimensional ideal fluid and a line sink, respectively. Flow forces acting on the molecular aggregates, elongated in shape, can be calculated from the velocity gradient tensor. The orientation of the aggregates is determined from the balance between the flow force and the disturbance due to the rotary Brownian motion, resulting in the Boltzmann distribution of identical form with Eq. (8), the width of the distribution being given as follows:

$$1/2\sin^2\delta=\zeta G/k_BT\ . \tag{9}$$

Here k_B and T represent the Boltzmann constant and temperature, respectively. ζ is the effective rotatory friction coefficient and G corresponds to the eigenvalue of the velocity gradient tensor. The local stress ζG is given as a sum of two terms, assuming a Bingham fluid, considering the plasticity of the monolayer;

$$\zeta G=\zeta'(4/\pi)(v_d/a)(1-4x^2/a^2)^{-1}+\tau_0\ . \tag{10}$$

The first term on the right-hand side is a Newtonian term proportional to the velocity gradient. ζ' shows a Newtonian friction coefficient. v_d and a show the dipping velocity and the width of the substrate, respectively. $x\,(-a/2\le x\le a/2)$ denotes the position relative to the center of the substrate, along the direction perpendicular to the dipping direction. The second term τ_0 is a constant denoting the Bingham yield value, below which the fluid behaves like an elastic body.

The term v_d/a in Eq. (10), combined with Eqs. (8) and (9), predicts the higher degree orientation, i.e., the small-

er value of δ, for the higher dipping velocity or narrower substrate width. The dependence of the local orientation on the substrate position originates from the term $(1-4x^2/a^2)^{-1}$ in Eq. (10). The higher degree of orientation is expected toward the edge of the substrate, that is, $x \rightarrow \pm a/2$. The dependence of the molecular orientation on these parameters, v_d/a and x/a, was actually observed by the optical study.[11] The optical absorbance of the system for the given direction of the electric vector of incident light is, in the first approximation, given by averaging the square of the direction cosine of the transition dipole moment of molecules.[22,23] The dichroic ratio R defined as the ratio of the absorbance for the electric vector parallel and perpendicular to the dipping direction, can be calculated using the distribution function defined in Eqs. (8)–(10) as

$$R=[I_0(\zeta G/2k_BT)+I_1(\zeta G/2k_BT)\cos 2\alpha]/[I_0(\zeta G/2k_BT)-I_1(\zeta G/2k_BT)\cos 2\alpha]\ . \tag{11}$$

Here I_0 and I_1 are the modified Bessel function of the zeroth and the first orders, respectively, and α is the angle between the dipping direction, which is parallel to the long axis of the J aggregate, and the transition dipole moment as defined in Fig. 2. By analyzing the dependence of the optical dichroic ratio of the J band on the substrate position in the DS films prepared with various values of v_d and a,[11] good agreement between theory and experiment was obtained and the parameter values were determined as follows: $\zeta'=5.0\times10^{-20}$ kg m^2 s^{-1} and $\tau_0=6.2\times10^{-21}$ kg m^2 s^{-2} in Eq. (11) and $\alpha=33.5°$.

Since the characteristic in-plane orientation of radical molecules, shown in FIg. 3, obtained by previous ESR studies[3–5] strongly suggests that the radicals originate from the molecules in the flow-oriented J aggregates, similar dependence of the orientation of radical molecules on the parameters v_d/a and x/a is expected. In the case of optical absorbance, the dependence of R on v_d/a and x/a was found to be well reproduced by Eq. (11) and the least-squares fitting of the data yielded the parameter values of ζ', τ_0, and α as described above. It is obvious, however, that the single datum of R obtained for particular values of v_d/a and x/a cannot yield the unique determination of two independent values of ζG and α in Eq. (11). On the other hand, ESR is a powerful method which can determine the distribution function of any sample, with any values of v_d/a and x/a in this case, through the spectrum simulation method[23] and henceforth simultaneously yields the values of δ and ϕ_0 in Eq. (8), which provides the independent determination of $\zeta G(=k_BT/2\sin^2\delta)$ and $\alpha(=90°-\phi_0)$.

Of particular importance is the observation of the local variation of δ expected from the first term of the right-hand side in Eq. (10), since the effect can be studied in a single sample and therefore the result is not affected by the sample dependent variation of ϕ_0, which will be discussed later. Figure 7 shows the value of δ as a function of x/a calculated from Eqs. (9) and (10) for two different cases of v_d/a employed in the measurements shown in Figs. 8 and 9. The upper curve corresponds to the case of $a=13$ mm and $v_d=50$ mm/min and the lower one to $a=13$ mm and $v_d=100$ mm/min. These curves are applicable to the different values of v_d or a, as long as the ratio v_d/a is being kept the same. As discussed above, δ decreases toward the edge of the substrate.

Solid curves in Fig. 8 show an example of the dependence of the ESR signal on the substrate position in a ^{15}N-enriched DS film prepared with $a=13$ mm and $v_d=50$ mm/min. Similarly the curves in Fig. 9 show the results in a film prepared with $a=13$ mm and $v_d=100$ mm/min. For both figures the external field lies in the film plane and is perpendicular to the dipping direction of the substrate. Data were recorded with a microwave power of 2 mW at room temperature. In each figure, the values of x at the center of a substrate of a 2-mm width at 5, 3, and 1 mm for the top, middle, and bottom curves, respectively. The local variation of ESR signal is most clearly recognized as the variation of the relative intensity of the shoulder marked by an arrow in each curve. The intensity of the shoulder reflects the relative intensity

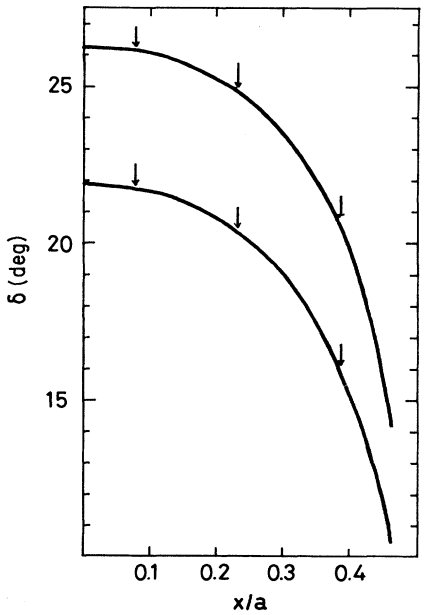

FIG. 7. The calculated value of δ as a function of x/a for two values of v_d/a using Eqs. (9) and (10). The upper curve corresponds to the substrate width of $a=13$ mm and the dipping velocity of $v_d=50$ mm/min, used for the data in Fig. 8 and the lower curve to $a=13$ mm and $v_d=100$ mm/min, used in Fig. 9. Three arrows in each curve correspond to $x=1$, 3, and 5 mm from left to right, for which the ESR spectra are shown in Figs. 8 and 9.

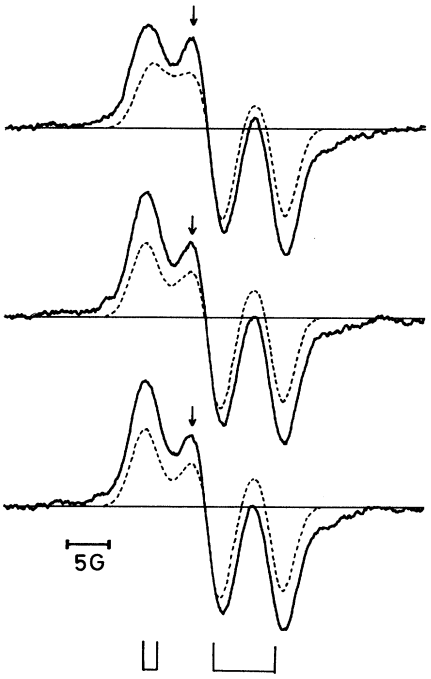

FIG. 8. Dependence of first-derivative ESR spectra on the substrate position in a 150-layered mixed LB film of ^{15}N-substituted DS and arachidic acid prepared with $a=13$ mm and $v_d=50$ mm/min (solid curves). External magnetic field lies in the film plane and is perpendicular to the dipping direction of the substrate. The values of x in Eq. (10) at the center of 2-mm-wide substrates are 5, 3, and 1 mm for the top, middle, and the bottom curves, respectively. Dashed lines show the simulated curves of the spin species A using the estimated value of δ in Eq. (8) calculated from Eq. (10). Stick lines at the bottom of the figure show the resonance fields due to the principal components of g and nitrogen hyperfine tensors.

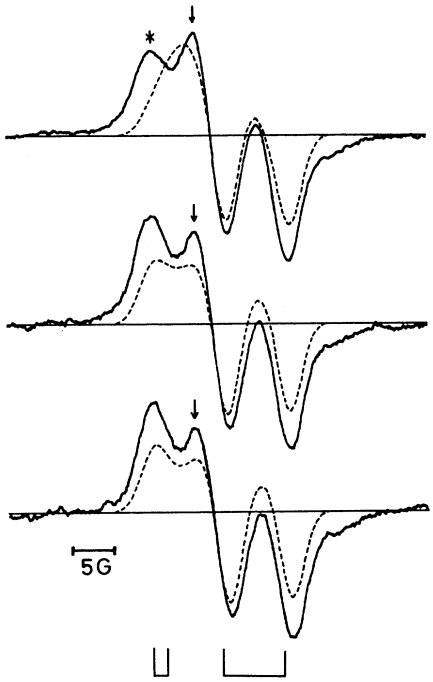

FIG. 9. Similar dependence of observed (solid line) and calculated (dashed line) first-derivative ESR spectra on the substrate position as Fig. 8 in a ^{15}N-substituted film prepared with $v_d=100$ mm/min. The values of x in Eq. (10) at the center of 2-mm-wide substrates are 5, 3, and 1 mm for the top, middle, and the bottom curves, respectively.

of the resolved doublet hyperfine structure of ^{15}N nucleus along the z axis, marked by stick lines at the bottom of each figure, and henceforth reflects the degree of orientation of the z axis along this direction of magnetic field.

The dashed curve in Fig. 8 shows the calculated ESR line shape with the value of δ in Eq. (8) being theoretically calculated from Eqs. (9) and (10); $\delta=26°$, 25°, and 21° for $x=1$, 3, and 5 mm, respectively, using $\zeta'=5.0\times10^{-20}$ kg m^2 s^{-1} and $\tau_0=6.2\times10^{-21}$ kg m^2 s^{-2} in Eq. (10). As mentioned above, these values of ζ' and τ_0 were obtained from the analysis of the flow dichroism of the J band in the optical absorption spectra,[11] and therefore account for the angular distribution function of the majority of molecules forming J aggregates. The value of $\phi_0=58.5°$ is chosen so as to reproduce the observed curves as close as possible.

The line-shape variation according to the position of the substrate is reasonably reproduced by the theoretically predicted values of δ. That is, the intensity of the resolved doublet structure increases toward the edge of the substrate, which can be recognized as the relative increase of the intensity of the shoulder marked by the arrow. This results from the higher degree of orientation toward the edge. It should also be noted that the intensity change of the doublet structure by a given shift of the substrate position is more prominent for the edge, from $x=3$ mm to 5 mm, than the center, from 1 mm to 3 mm, which is well understood from the functional form $(1-4x^2/a^2)^{-1}$. The consideration of the variation of δ within a 2-mm-wide substrate, according to Eq. (10), does not significantly modify the calculated curve shown in Fig. 8, using the value of δ corresponding to the center of the 2-mm-wide substrate. We also note here that the apparent difference between the observed and calculated line shapes is mostly resolved if we consider the overlapping signal from species B. The agreement between the observed and calculated curves obtained here for the ^{15}N-substituted sample, prepared with $a=13$ mm and $v_d=50$ mm/min, coincides well with the case for the unsubstituted sample, prepared with the same condition, reported in Ref. 12.

The dashed curve in Fig. 9 similarly shows the calculated spectra. In this case, the values of $\delta=22°$, 20°, and 16° are calculated for $x=1$ mm, 3 mm, and 5 mm, respectively. The smaller values of δ compared with the above case reflects the higher dipping velocity of $v_d=100$ mm/min employed in this case. As a result, the relative intensity of the doublet structure indicated by arrows is

more pronounced in the curves in Fig. 9 than in those in Fig. 8, reflecting the higher degree of orientation. Although the general tendency of the line-shape variation is reproduced fairly well also in this case, there is a discrepancy between the observed and calculated curves, which become more clearly recognized for the top curve than the other two curves. This situation again coincides well with the case for the unsubstituted sample prepared with the same condition.[13] A possible cause for the discrepancy will be discussed later.

The enhanced degree of orientation for the higher dipping velocity observed by ESR is also well demonstrated in the optical dichroism of J band. Figure 10 shows an example of the anisotropy of the optical absorption taken at the center of the substrate in 4-layered ^{15}N-substituted DS films, for a sample prepared with $a=13$ mm and $v_d=50$ mm/min in Fig. 10(a) and that with $a=13$ mm and $v_d=100$ mm/min in Fig. 10(b). The spectral line

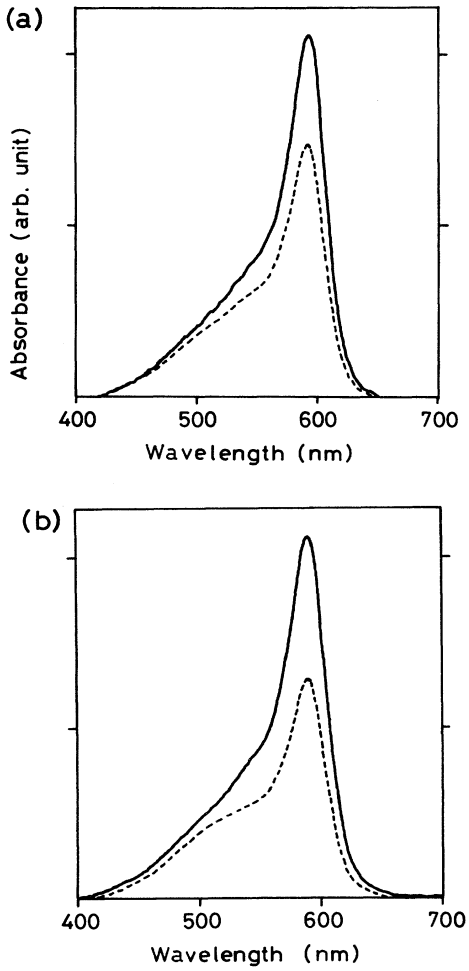

FIG. 10. Dependence of the in-plane optical dishroism of ^{15}N-substituted DS films on the dipping velocity. Specimens are 4-layered films prepared with the substrate width of $a=13$ mm and the dipping velocity of $v_d=50$ mm/min for (a) and $v_d=100$ mm/min for (b). The solid and the dashed lines correspond to the electric vector parallel and perpendicular to the dipping direction, respectively.

shape associated with the J band of ^{15}N-substiuted samples coincide with that of unsubstituted samples.[4,11] In both figures, the polarization vector lies in the film plane and parallel to the dipping direction of the substrate for the solid curves and perpendicular to the dipping direction for the dotted curves, respectively. As seen from the figure, the dichroic ratio R is larger for the case of Fig. 10(b) with a higher dipping velocity. The observed dichroic ratios of 1.43 in the case of Fig. 10(a) and 1.65 in Fig. 10(b) coincide with the previous results in 10-layered or thicker unsubstituted films prepared with corresponding values of a and v_d within an experimental error. The effect of layer thickness on the value of R was found to be almost negligible for the films thicker than 4 monolayers in the present system.

Incidentally, if the ESR anisotropy and optical dichroism keep a good correlation, as demonstrated here, the sample dependence of ϕ_0 observed in ESR, as pointed in Sec. IV, should result in the corresponding variation of optical dichroic ratio R. One typical example is that the initially obtained ^{15}N-substituted film prepared with $a=13$ mm and $v_d=50$ mm/min^{-1} showed a considerably high value of $R=2.8$ without change of the J-band peak position, compared with $R=1.43$ for the film prepared with the same condition shown in Fig. 10(a). Correspondingly, the ESR spectrum showed a more resolved doublet structure with a larger value of $\phi_0=64°$. This is why the doublet structure of the spectra in Fig. 4 of Ref. 12, obtained at $x=5$ mm shows a much larger relative intensity compared with the bottom curve of Fig. 8, obtained under the same conditions of v_d/a and x/a. Although the observed value of $R=2.8$ is considerably larger than that calculated from $\phi_0=64°$ of $R\approx 2.0$, the result certainly shows the strong correlation between ϕ_0 and R. The variation of ϕ_0 may be related to the difference of the shape of two-dimensional crystallites containing DS and arachidic acid formed on the water surface, however, the problem is left open for further investigation.

As for the cause of the discrepancy between the observed and calculated curves in Fig. 9, it is noted that the discrepancy is most clearly recognized for the top curve in Fig. 9 as the appearance of the peak at $g=2.009$ along the y axis in the observed curve (marked by an asterisk), which lacks in the calculated curve. Since this peak becomes more prominent as the degree of orientation becomes lower, which can be seen from the comparison of the calculated curves in Figs. 8 and 9, the prominence of the peak may indicate the increase of poorly oriented or unoriented domains. Preliminary calculation incorporating the effect of unoriented domains showed that the intensity of the peak at $g=2.009$ can be enhanced by such effect. Such unoriented domains may be produced toward the edge of substrate, where the shearing stress diverges in the present model.[10,11] Although the divergence at the edge is unrealistic, the higher shearing stress may cause the degradation of the film structure, resulting in the increase of an unoriented portion. More detailed discussion of this edge effect is beyond the scope of this paper.

Despite the above-mentioned minor discrepancy, it

should be emphasized that both the local orientations of the radicals and the majority of molecules forming J aggregates are well described by the theory of flow orientation where the degree of the orientation is governed by the parameters of v_d/a and x/a. This detailed coincidence between the orientation of radical molecules and that of the majority of molecules forming J aggregates provides new important evidence that the radicals have their origin in J aggregates.

C. Origin of stable radicals—possibility of intermolecular charge transfer in J aggregates

We have previously proposed an intermolecular charge transfer model for the mechanism of the radical generation.[1-5] As mentioned in Sec. I, ESR spectra contain the signals from two radical species, A and B, of comparable spin concentration in the dark condition. Their ESR intensities seem to be simultaneously enhanced under illumination.[2,4] These facts strongly suggest that the observed radicals are the cation and anion radicals generated by an intermolecular charge transfer in J aggregates.

In this model, the wave functions of the radicals should coincide with HOMO and LUMO of the dye molecule.[4] The detection of the nitrogen coupling in benzothiazole of the present study shows that the radical wave function is directly associated with the dye chromophore, N—C=C—C=C—C=O, on which electron densities of HOMO or LUMO are expected. The observed hyperfine coupling along the z axis of 5.4 G in the case of the ^{14}N sample gives an estimation of the spin density on the nitrogen of $\rho_N \approx 0.2$, using the linear relation between the hyperfine coupling and spin density; $A_{\text{obs}} = A_N \rho_N$ with $A_N = 32$ G for the ^{14}N nucleus.[17] The location of spin density other than the nitrogen may be further studied by isotope substitution of relevant nuclear spin sites.

As for species B, observed g values are consistent with those of π-electron radical. It should also be pointed out that the observed spectral of species B show distinct anisotropy, which is clearly recognized by the difference of spectral region between Figs. 2(a) and 2(c), showing that the species B is also an oriented π-electron radical. The spectral width with no resolved structures of species B may be consistent with the situation of distributed spin density on the molecular skeleton, giving rise to the unresolved hyperfine structure due to protons and nitrogen atoms. Concerning this point, contrary to the case of species A, no distinct spectral change of species B was observed by the substitution of ^{15}N. This situation becomes clear if we notice from Figs. 5 and 6 that the higher-field tail of the spectra due to species B is recognized both at the X and K bands in ^{15}N-subsituted and unsubstituted films without significant change. Thus no large spin density exists on the nitrogen in benzothiazole in the case of species B and the linewidth may arise from other nuclear spin sites. It would be useful to use the isotope substitution of relevant nuclear sites to reveal the wave function of species B.

Although the molecular orbitals of radical species A and B are not yet completely clear at present, it should be emphasized that the generation of these stable radical species is a new phenomenon associated with J aggregates formed as monolayer assemblies in LB films and the observed nitrogen spin density is expected to probe the electronic states of dye molecules in the aggregated state.

In conclusion, we have made ESR studies of the stable radicals, species A and B, existing in the mixed Langmuir-Blodgett films of a merocyanine dye and arachidic acid. Comparison of the spectra of the films using ^{15}N-subsituted and unsubstituted dyes identified the observed hyperfine structure of species A to be arising from the nitrogen in the dye chromophore. ESR spectrum simulation method considering the three-dimensional freedom of orientation was developed to analyze molecular orientations and its validity was confirmed by applying the method to reproduce the frequency dependence of the spectra at X and K bands using the same parameter values for angular distribution function. Positional dependence of the ESR spectra in the substrate was analyzed and the local orientation of the radical species A showed a higher degree of orientation towards the edge of the substrate. The behavior coincides well with that of the majority of dye molecules forming J aggregates deduced from optical analysis, and is well described by the recent theory of flow orientation during the LB dipping process. The coincidence provides new evidence that the radicals originate from J aggregates. Further work is suggested to examine the possibility of the assignment of the radicals A and B to either the cation or anion of the dye molecules, as previously proposed by the model of intermolecular charge transfer in J aggregates, through the study of the molecular orbitals of these radicals by identifying possible hyperfine couplings.

ACKNOWLEDGMENTS

The present authors thank Dr. S. Yasui for the synthesis of the merocyanine dyes.

[1] S. Kuroda, M. Sugi, and S. Iizima, Thin Solid Films **99**, 21 (1983).
[2] S. Kuroda, M. Sugi, and S. Iizima, Thin Solid Films **133**, 189 (1985).
[3] S. Kuroda, K. Ikegami, M. Sugi, and S. Iizima, Solid State Commun. **58**, 493 (1986).
[4] S. Kuroda, K. Ikegami, K. Saito, M. Saito, and M. Sugi, J. Phys. Soc. Jpn. **56**, 3319 (1987).
[5] S. Kuroda, K. Ikegami, K. Saito, M. Saito, and M. Sugi, Thin Solid Films **159**, 285 (1988).
[6] M. Sugi and S. Iizima, Thin Solid Films **68**, 199 (1980).
[7] V. Czikkely, H. D. Försterling, and H. Kuhn, Chem. Phys. Lett. **6**, 11 (1970); **6**, 207 (1970).
[8] T. Fukui, M. Saito, M. Sugi, and S. Iizima, Thin Solid Films **109**, 247 (1980).
[9] H. Nakahara, K. Fukuda, D. Möbius, and H. Kuhn, J. Phys. Chem. **90**, 6144 (1986).
[10] N. Minari, K. Ikegami, S. Kuroda, K. Saito, M. Saito, and M. Sugi, Solid State Commun. **65**, 1259 (1988).
[11] N. Minari, K. Ikegami, S. Kuroda, K. Saito, M. Saito, and M. Sugi, J. Phys. Soc. Jpn. **58**, 222 (1989).
[12] S Kuroda, K. Ikegami, K. Saito, M. Saito, M. Sugi, S. Suga,

and S. Yasui, Solid State Commun. **71**, 333 (1989).
[13]S. Kuroda, K. Ikegami, K. Saito, M. Saito, and M. Sugi, Thin Solid Films **178**, 555 (1989).
[14]J. Messier and G. Marc, J. Phys. (Paris) **32**, 799 (1971).
[15]P. A. Chollet, J. Phys. C **7**, 4127 (1974).
[16]M. Vandevyver, A. Barraud, A. Ruaudel-Teixier, P. Maillard, and C. Gianotti, J. Colloid Interface Sci. **85**, 571 (1982).
[17]J. R. Morton, Chem. Rev. **64**, 453 (1964).
[18]J. E. Wertz and J. R. Bolton, *Electron Spin Resonance* (McGraw-Hill, New York, 1972), Chap. 3.
[19]Table C of Ref. 18.
[20]"the peak-to-peak width of 1.8 *G*" at line 5, p. 189 of Ref. 5 should read as "the half width at half maximum (of integrated form) of 1.8 *G*."
[21]S. Nishikawa, Y. Tokura, T. Koda, and K. Iriyama, Jpn. J. Appl. Phys. **25**, L701 (1986).
[22]J. Breton, M. Michel-Villaz, G. Paillotin, and M. Vandevyver, Thin Solid Films **13**, 351 (1972).
[23]M. Vandevyver and A. Barraud, J. Mol. Electron **4**, 207 (1988).